Quaternary Science Reviews 123 (2015) 16–30

Contents lists available at ScienceDirect

Quaternary Science Reviews

journal homepage: www.elsevier.com/locate/quascirev

Precession and obliquity forcing of the freshwater budget over the Mediterranean

J.H.C. Bosmans [a, b, *], S.S. Drijfhout [b, 1], E. Tuenter [a, b], F.J. Hilgen [a], L.J. Lourens [a], E.J. Rohling [c]

[a] Utrecht University, Faculty of Geosciences, Department of Earth Sciences, Budapestlaan 4, 3584 CD, Utrecht, Netherlands
[b] Royal Netherlands Meteorological Institute, Postbus 201, 3730 AE, De Bilt, Netherlands
[c] The Australian National University, Research School of Earth Sciences, Canberra, ACT 2601, Australia

ARTICLE INFO

Article history:
Received 22 September 2014
Received in revised form
12 May 2015
Accepted 8 June 2015
Available online 23 June 2015

Keywords:
Mediterranean
Paleoclimate modelling
Orbital forcing (precession, obliquity)
Freshwater

ABSTRACT

There is strong proxy and model evidence of precession- and obliquity-induced changes in the freshwater budget over the Mediterranean Sea and its borderlands, yet explanations for these changes vary greatly. We investigate the separate precession and obliquity forcing of the freshwater budget over the Mediterranean using a high-resolution coupled climate model, EC-Earth. At times of enhanced insolation seasonality, i.e. minimum precession and maximum obliquity, the area was wetter and the Mediterranean Sea surface was less saline. The latter has been attributed to increased runoff from the south as a consequence of a strengthened North African monsoon, as well as to increased precipitation over the Mediterranean Sea itself. Our results show that both mechanisms play a role in changing the freshwater budget. Increased monsoon runoff occurs in summer during times of enhanced insolation seasonality, especially minimum precession, while increased precipitation is important in winter for both precession and obliquity. We relate changes in winter precipitation to changes in the air-sea temperature difference and subsequently, convective precipitation. The freshening in the minimum precession and maximum obliquity experiments has a strong effect on Mediterranean sea surface salinity and mixed layer depth, thereby likely influencing deep sea circulation and sedimentation at the ocean bottom.

1. Introduction

The response of Mediterranean climate to orbital forcing is a heavily debated topic in paleoclimatology. A large body of data has shown that at times of enhanced insolation seasonality, i.e. minimum precession and maximum obliquity, the Mediterranean area was wetter and the Mediterranean Sea surface freshwater budget (evaporation minus precipitation and runoff) was reduced. As a consequence of reduced surface buoyancy loss, deep water ventilation was weakened and dark, organic-rich layers formed on the sea floor. Rossignol-Strick (1985) proposed a physical link between the occurrence of these so-called sapropels and orbitally forced increases in North African monsoon strength, which consequently strengthens Nile river runoff. Although the sapropels are mainly paced by precession, an obliquity pattern is present as well (e.g. Lourens et al., 1996).

The strengthening of the North African monsoon during times of increased insolation seasonality, such as minimum precession and maximum obliquity, has been confirmed by many studies (Kutzbach et al., 2013; Bosmans et al., 2015; Larrasoaña et al., 2013, and references therein). The subsequent increase in runoff towards the Mediterranean holds as the most widely adopted hypothesis for the formation of sapropels, appearing in handbooks on paleoclimatology (Ruddiman, 2007). However, other components of the Mediterranean climate may have played a role as well. Increased precipitation over the basin itself at times of increased summer insolation has been related to increased summer precipitation (Rossignol-Strick, 1987; Rohling and Hilgen, 1991; Rohling, 1994). This idea has however largely been abandoned; recent

* Corresponding author. Present address: Utrecht University, Faculty of Geosciences, Department of Physical Geography, Heidelberglaan 2, 3584 CS, Utrecht, Netherlands.
E-mail address: J.H.C.Bosmans@uu.nl (J.H.C. Bosmans).
[1] Also at: University of Southampton, Ocean and Earth Sciences, Waterfront Campus (NOCS), European Way, Southampton SO14 3ZH, United Kingdom.

http://dx.doi.org/10.1016/j.quascirev.2015.06.008
0277-3791/

palynological, lake isotopic and lake-level studies point to summer aridity (e.g. Tzedakis, 2007, 2009). Hence wetter conditions over the Mediterranean basin must be related to increased winter precipitation, often attributed to increased Mediterranean storm track activity (e.g. Tzedakis, 2007; Brayshaw et al., 2011; Kutzbach et al., 2013). Furthermore, strong similarities between the sapropel record in the Mediterranean and sedimentary sequences in western Spain and Morocco suggests that both respond to orbital forcing in similar ways (van der Laan et al., 2012). Atlantic storm tracks affect both western Spain and Morocco and can induce increased storm activity over the Mediterranean, hence increased storm track activity could explain wetter conditions at times of increased insolation seasonality in both regions. Increased (net) precipitation over the Mediterranean basin and increased river runoff from the northern borderlands of the Mediterranean may be of equal or greater importance than increased Nile river runoff in changing the freshwater budget, as the former two freshwater sources are situated more favourably in terms of location and timing of the deep water ventilation (Meijer and Tuenter, 2007).

To summarise, orbitally forced changes in the Mediterranean freshwater budget, and therefore sapropel formation, have been attributed to various sources (e.g. Tzedakis, 2007, 2009; Rohling et al., 2009; Kutzbach et al., 2013). The model study by Kutzbach et al. (2013) states that not only monsoon runoff but also winter precipitation over the Mediterranean at times of a precession minimum could explain humid periods in paleoclimatic records, but give no comparison of precipitation and runoff amounts. Meijer and Tuenter (2007) showed the relative roles of (net) precipitation and runoff from both north and south, but based their result on a low resolution intermediate complexity model. Both studies focus on precession forcing, while obliquity leaves an imprint on the sapropel record as well (Lourens et al., 1996). In this study, we use for the first time a high-resolution general circulation model, EC-Earth, to investigate changes in the Mediterranean freshwater budget due to changes in both precession and obliquity. Specifically, we aim to determine the relative roles of precipitation, evaporation and runoff over/into the basin. Also, we examine the causes behind changes in these freshwater budget terms, in order to determine whether changes in the Mediterranean freshwater budget are mainly driven by the North African monsoon, (Atlantic) storm tracks or local changes.

This paper starts with an overview of the model, EC-Earth, and a description of the experimental design (Section 2). We then briefly discuss the freshwater budget in a pre-industrial control experiment in Section 3.1, as an evaluation of EC-Earth's capability of modelling Mediterranean climate. The main results are shown in Sections 3.2, 3.3 and 3.4, where we examine changes in (net) precipitation and runoff as well as possible causes. We also briefly touch upon the possible effects of the freshwater budget changes on deep water formation in Section 3.5. Section 4 provides a discussion in which we compare our results to both proxy data and model studies. A conclusion is given in Section 5.

2. Model and experiment set-up

2.1. EC-earth

EC-Earth is a fully coupled ocean-atmosphere GCM (general circulation model). Here we use version 2.2, based on the Integrated Forecasting System (IFS), cycle 31R1 of the European Centre for Medium-range Weather Forecast (ECMWF), running at a resolution of roughly 1.125° × 1.125° (T159) with 62 vertical levels. For more details see Hazeleger et al. (2010, 2011). Dynamic vegetation is not included. The ocean component consists of NEMO (Nucleus for European Modelling of the Ocean), version 2, running at a horizontal resolution of nominally 1° with 42 vertical levels (Madec 2008; Sterl et al., 2011). For the vertical levels a z-coordinate is used with thickness increasing from 10 m at the surface to 100–300 m at depth. The Mediterranean consists of 363 surface gridboxes in the horizontal on a curvilinear C-grid. NEMO incorporates the sea-ice model LIM2. The ocean, sea-ice, land and atmosphere modules are coupled through the OASIS3 coupler (Valcke and Morel, 2006).

The same version of EC-Earth was shown to reproduce Mid-Holocene monsoon precipitation well compared to PMIP2 model studies (Bosmans et al., 2012). Furthermore, in the precession and obliquity experiments that are also used in this study, the North African monsoon was shown to respond strongly to the insolation forcing, being mainly driven by enhanced moisture transport from the Atlantic (Bosmans et al., 2015). This is in line with recent GCM studies (e.g. Herold and Lohmann, 2009) but in contrast to previous intermediate complexity model studies such as that of Tuenter et al. (2003), which showed a distinctively different source of moisture. Hence the state-of-the-art model EC-Earth has already provided new paleoclimatological insights.

2.2. Experiments

In this study we use four idealized experiments in which the precession and obliquity effects can be studied separately. These experiments were also used in Bosmans et al. (2015). The orbital configuration used in each experiment is summarised in Table 1.

During minimum precession (Pmin), when the precession parameter $e \sin(\pi + \tilde{\omega})$ is at its minimum value, Northern Hemisphere summer solstice occurs at perihelion (the point closest to the Sun). Seasonality of insolation is enhanced on the Northern Hemisphere and decreased on the Southern Hemisphere. During maximum precession (Pmax), Southern Hemisphere summer occurs at perihelion. Insolation differences at ~ 40° N are on the order of 100 Wm^{-2} for precession and 15 Wm^{-2} for obliquity with opposite anomalies in summer and winter (see Fig. 1 in Tuenter et al. (2003) or Bosmans et al. (2015)). Only orbital parameters, and thus insolation, vary amongst the experiments; all other boundary conditions (e.g. greenhouse gasses, ice caps) are kept at pre-industrial values, as is the calendar. More details can be found in Bosmans et al. (2015). Furthermore, we briefly discuss a pre-industrial control experiment using boundary conditions as prescribed by the Paleoclimate Modelling Intercomparision Project (see http://pmip3.lsce.ipsl.fr). This pre-industrial experiment is described in Bosmans et al. (2012).

In this study we compare Pmin with Pmax, and Tmax with Tmin, i.e. we investigate the effect of increased summer and decreased winter insolation. These experiments were initiated from a pre-industrial control experiment. Each experiment is run for 100 years, of which the last 50 years are used to create the climatologies shown in this study. This is long enough for atmospheric and surface variables that are of interest to equilibrate to the forcing (see Bosmans et al. (2015)). The globally averaged tendency term of

Table 1
Overview of the orbital configuration in each experiment. Obl is the obliquity (tilt), $\tilde{\omega}$ is the longitude of perihelion, defined as the angle from the vernal equinox and perihelion, measured counterclockwise. e is eccentricity. $e \sin(\pi + \tilde{\omega})$ is the precession parameter. Note that for Tmax and Tmin there is no precession because of the circular orbit ($e = 0$).

Experiment	Obl (°)	$\tilde{\omega}$ (°)	e	$e \sin(\pi + \tilde{\omega})$
Pmin	22.08	95.96	0.056	−0.055
Pmax	22.08	273.5	0.058	0.058
Tmax	24.45	–	0	0
Tmin	22.08	–	0	0

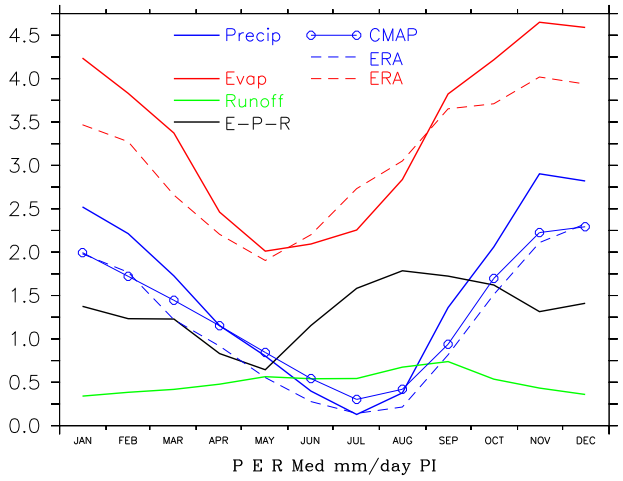

Fig. 1. Precipitation, evaporation, runoff and E-P-R (net loss) over the Mediterranean Sea for the EC-Earth pre-industrial experiment (solid lines), CMAP (open dots, Xie and Arkin (1997)) and ERAinterim (dashed, Dee et al. (2011)) in mm/day. Only gridpoints over the Mediterranean Sea are taken into account.

surface air temperature, dT/dt, is near-zero and shows no trend in all experiments (not shown).

In order to investigate changes in the freshwater fluxes over the Mediterranean Sea, we discuss precipitation, evaporation and runoff. In EC-Earth, the land area is divided in drainage basins, four of which drain into the Mediterranean: the northern borderlands of the Mediterranean (Southern Europe and part of the Middle East), the Nile, the northern Sahara and the Chad basin (Fig. 5(c)). The Chad basin is at present an endorheic (closed) basin, draining in continental Lake Chad. EC-Earth, however, does not contain a lake model and therefore runoff from the Chad basin has to be routed to an ocean to close the global water budget. In EC-Earth the Chad runoff is routed to the Mediterranean (the Gulf of Sirte). In this study we use pre-industrial boundary conditions and therefore subtract Chad runoff when discussing the freshwater fluxes in Sections 3.1–3.4 and Fig. 4. Accordingly, in these Sections/Figures, runoff from the south into the Mediterranean Sea is composed of runoff from the Sahara and Nile basins (Fig. 5). In Section 3.5 we briefly discuss the effects of changes in the freshwater fluxes on ocean circulation, which responds to the full freshwater flux including Chad runoff (so the effect of this runoff into the Gulf of Sirte is for instance visible in the salinity changes, Fig. 11(a) and (b)).

3. Results

3.1. Pre-industrial (control run)

Here we briefly describe the Mediterranean freshwater budget (precipitation, evaporation and runoff) for the pre-industrial control experiment, before discussing the orbital-induced changes in the next sections. Fig. 1 shows that EC-Earth reproduces a typical Mediterranean climate over the basin, with evaporation dominating the freshwater budget, as well as dry summers and runoff peaking in late summer/early autumn (when monsoon runoff reaches the Nile delta). Summer drought over the Mediterranean is related to sub-tropical high-pressure conditions, which move southward during winter. The Mediterranean area then becomes affected by the temperate westerlies and associated Atlantic depressions. Such depressions may bring precipitation by continuing their track into the Mediterranean. However, most precipitation is sourced by evaporation from the Mediterranean Sea itself, through local convection and cyclones formed over the basin itself (e.g. Bengtsson et al., 2006; Rohling et al., 2015; Matthews et al., 2000). Yet, Mediterranean cyclones can be triggered by external sources such as the above mentioned Atlantic depressions that can induce new depressions over the Mediterranean, or inflow of cold and dry northerly air from Eurasia over the warm and wet Mediterranean Sea (e.g. Saaroni et al., 1996; Trigo et al., 1999; Xoplaki et al., 2004; Romem et al., 2007). For details on Mediterranean climatology and circulation see e.g. Lolis et al. (2002); Ulbrich et al. (2012); Kutzbach et al. (2013); Rohling et al. (2015). In the EC-Earth pre-industrial control experiment, winter precipitation and evaporation are slightly overestimated compared to the CMAP and ERA-Interim data sets (Xie and Arkin, 1997; Dee et al., 2011, respectively), while net evaporation (E-P) is slightly underestimated in summer (not shown).

The spatial variation in precipitation and evaporation is captured well in EC-Earth in both the summer and winter half year (Fig. 2). There is little summer precipitation over the Mediterranean Sea. Summer precipitation over the Balkan and southern France/northern Spain is slightly overestimated in EC-Earth compared to ERA-Interim. The location of winter precipitation is also captured well but is also higher in EC-Earth than in ERA-Interim, with most precipitation occurring over the Adriatic Sea, northern Levantine and southern Sea of Sardinia. These are areas where the temperature difference between the relatively warm sea surface and cool air is strong (not shown), leading to convective precipitation. Like winter precipitation, winter evaporation over the basin is also slightly overestimated (Figs. 1 and 2). Temperature patterns over the Mediterranean area are similar. Overall temperatures are lower in EC-Earth than ERA-Interim, see Fig. 3, which are likely due to EC-Earth reflecting pre-industrial conditions, while ERA-Interim reflects the present-day.

The components of the freshwater budget over the Mediterranean Sea in EC-Earth are summarised in Table 2. The annual mean evaporation and precipitation, 3.37 and 1.54 mm/day respectively, are slightly overestimated compared to CMAP and ERA-Interim (Fig. 1), but fit within the range of values given in literature (2.52–4.30 mm/day for evaporation, 0.71–1.92 mm/day for precipitation) based on observations and reanalyses (Criado-Aldeanueva et al., 2012; Adloff et al., 2011, and references therein). Annual mean river runoff is 0.44 mm/day, mostly coming from Southern Europe. This is close to, but slightly higher than, the 0.39 mm/day indicated by Ludwig et al. (2009).

The net loss (E-P-R) of 1.38 mm/day is compensated by inflow from the Atlantic and the Black Sea. The in- and outflow through the Strait of Gibraltar is overestimated (1.59 and 1.56 Sv in EC-Earth respectively, 1 Sv $= 10^6$ m^3/s, compared to 0.82 and 0.78 in Criado-Aldeanueva et al., 2012). This overestimation in the model is due to the strait being one gridbox wide, ~90 km, compared to its actual size of ~15 km (Sterl et al., 2011; Criado-Aldeanueva et al., 2012). The same problem affects the in- and outflow from the Black Sea, 0.144 and 0.138 Sv in EC-Earth respectively, compared to 0.038 and 0.03 Sv in Kanarska and Maderich (2008). The net inflow from the Atlantic, however, of 0.035 Sv fits well within the range of values in literature; the inflow from the Black Sea (0.006 Sv), is on the low end (Criado-Aldeanueva et al., 2012; Soto-Navarro et al., 2010, and references therein).

In total, the inflow of Atlantic and Black Sea water adds an annual mean of 1.37 mm/day to the Mediterranean Sea, which compensates the net loss through evaporation (E-P-R) of 1.38 mm/day (Table 2).

3.2. Basin-mean precession- and obliquity-induced changes

The annual- and basin-mean changes over the Mediterranean Sea, as summarised in Table 2, indicate a freshening in Pmin and

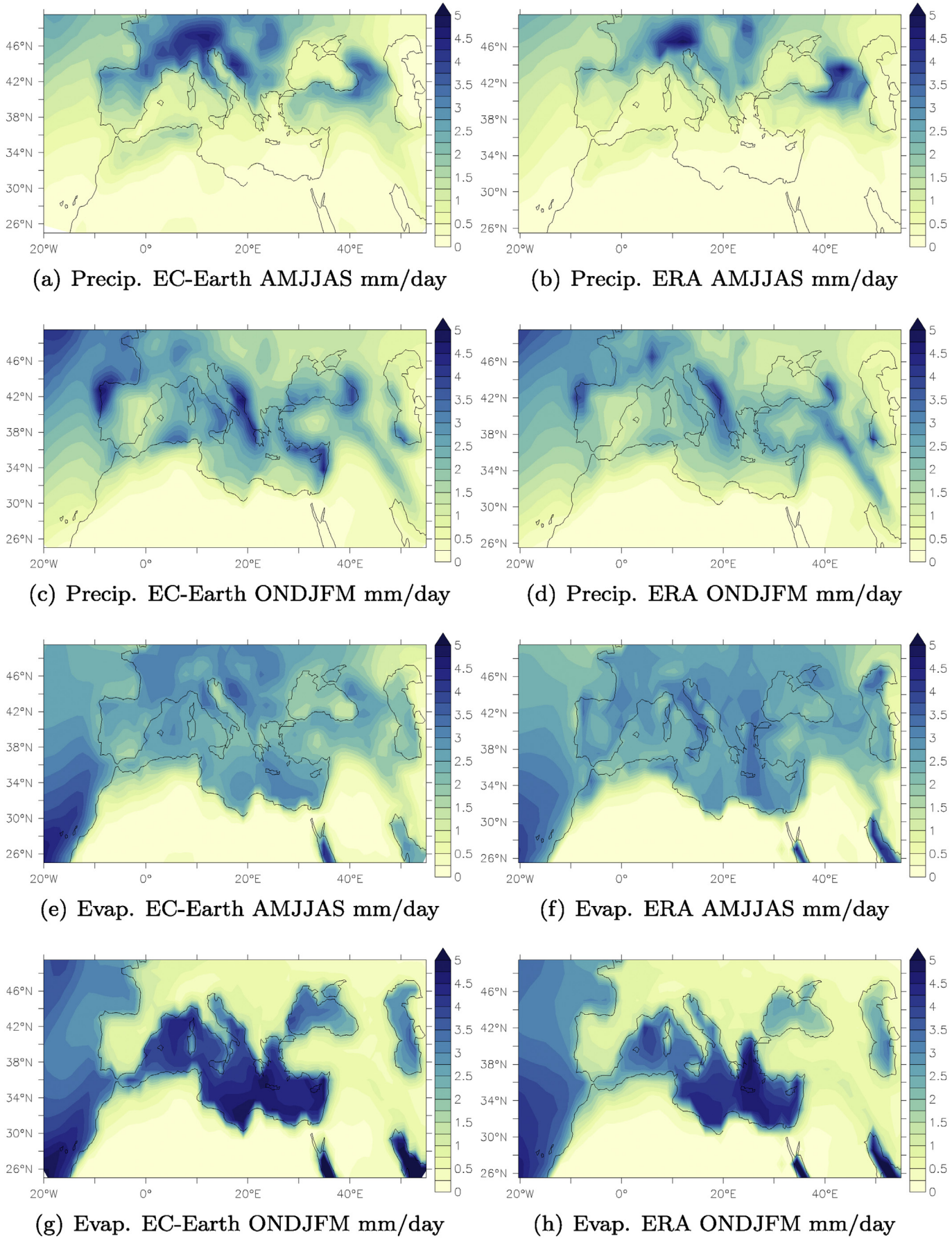

Fig. 2. Precipitation and evaporation in the EC-Earth pre-industrial experiment (left, a–c–e–g) and the ERA-Interim data set (right, b–d–f–h, Dee et al., 2011) for the summer half year (AMJJAS, a–b–e–f) and winter half year (ONDJFM, c–d–g–h).

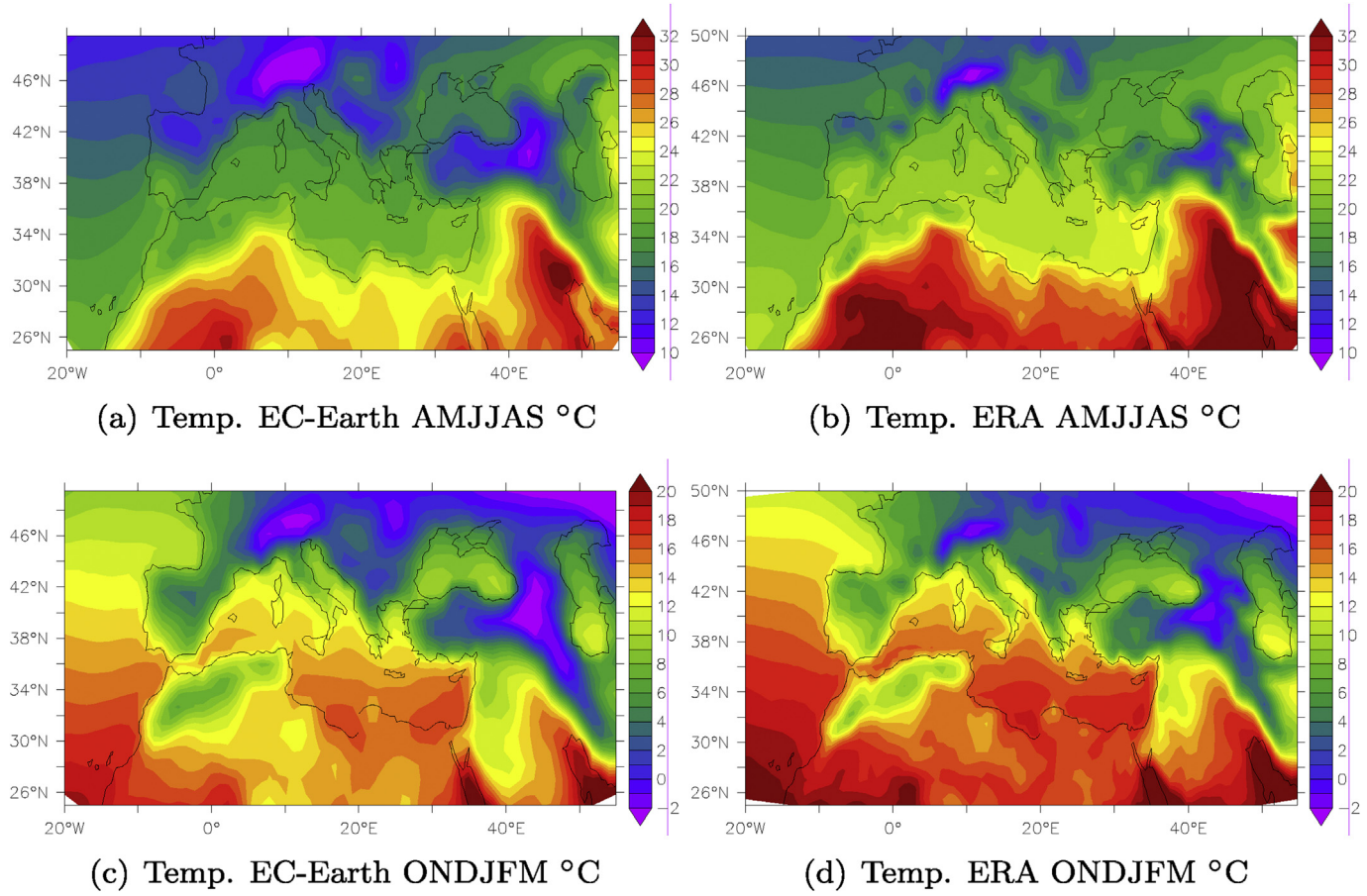

Fig. 3. Temperature (2 m above surface) in the EC-Earth pre-industrial experiment (left, a–c) and the ERA-Interim data set (right, b–d, Dee et al., 2011) for the summer half year (AMJJAS, a–b) and winter half year (ONDJFM, c–d). Note the different colour scales in a–b and c–d. (For interpretation of the references to colour in this figure legend, the reader is referred to the web version of this article.)

Tmax compared to Pmax and Tmin. For precession, the freshwater flux (P-E + R) is increased by 0.95 mm/day in Pmin, mostly due to increased runoff from the south (0.66 mm/day, from the Nile and Sahara basins). Increased precipitation adds another 0.22 mm/day while the annual-mean evaporation change is negligible. For obliquity, evaporation does not contribute either to the annual mean freshwater flux changes (Table 2). Precipitation over the basin is increased by 0.16 mm/day in Tmax, making the largest contribution to the 0.25 mm/day total change in freshwater flux, followed by runoff from the south (0.11 mm/day). Note that the change in runoff from the south is largest in terms of percentage.

The increase in precipitation over the basin is mostly due to increased precipitation in autumn and winter for both precession and obliquity (Fig. 4(a) and (b)). During summer precipitation is slightly decreased. For precession, this summer precipitation decrease is compensated by lower evaporation, so net precipitation (P-E) shows only small changes during summer (Fig. 4(c)). In autumn, increased evaporation overcompensates increased precipitation; P-E is reduced. In winter P-E shows the largest increase due to the combined effect of increased precipitation and decreased evaporation. The largest changes occur in February, when the precipitation increase is strongest. For obliquity, P-E is increased in nearly all months as precipitation changes are more positive than evaporation changes (Fig. 4(d)) and the largest changes occur in early winter, with precipitation change peaking in November.

Runoff is increased in all months, predominantly from the south (i.e. monsoonal) in summer and early autumn (Fig. 4(c) and (d)). This increase in runoff is mostly from the Nile river (runoff from the Chad basin is ignored in Fig. 3, see Section 2). There is a small increase in river runoff from Southern Europe in late winter/early spring in Pmin, and in winter for Tmax (Fig. 4(c) and (d)).

Hence there is an overall increase in the freshwater budget (P-E + R), dominated by runoff from the south in Pmin and by winter precipitation over the basin in Tmax. In the next sections we focus on the mechanisms behind these freshwater budget changes. First we briefly look at the summer half year (AMJJAS), then we focus on the changes in winter half year (net) precipitation, which dominate the changes in winter freshwater flux (winter half year: ONDJFM).

3.3. Summer

The increased runoff from the south in the Pmin and Tmax experiments is in line with a strengthening of the North African monsoon (Bosmans et al., 2015, and references therein). Increased monsoon precipitation results in increased surface runoff in the monsoon region, especially in the Nile and Chad drainage basins, see Fig. 5 and Table 2. Runoff changes are especially large between Pmin and Pmax, due to strong differences in monsoon strength between Pmin and Pmax (Bosmans et al., 2015). Runoff from the northern Mediterranean borderlands (Southern Europe) shows very little change compared to that from the North African monsoon region (see also Fig. 4).

Summer precipitation over the basin itself is lower in Pmin and Tmax (Fig. 4(a) and (b)). The increased summer insolation leads to

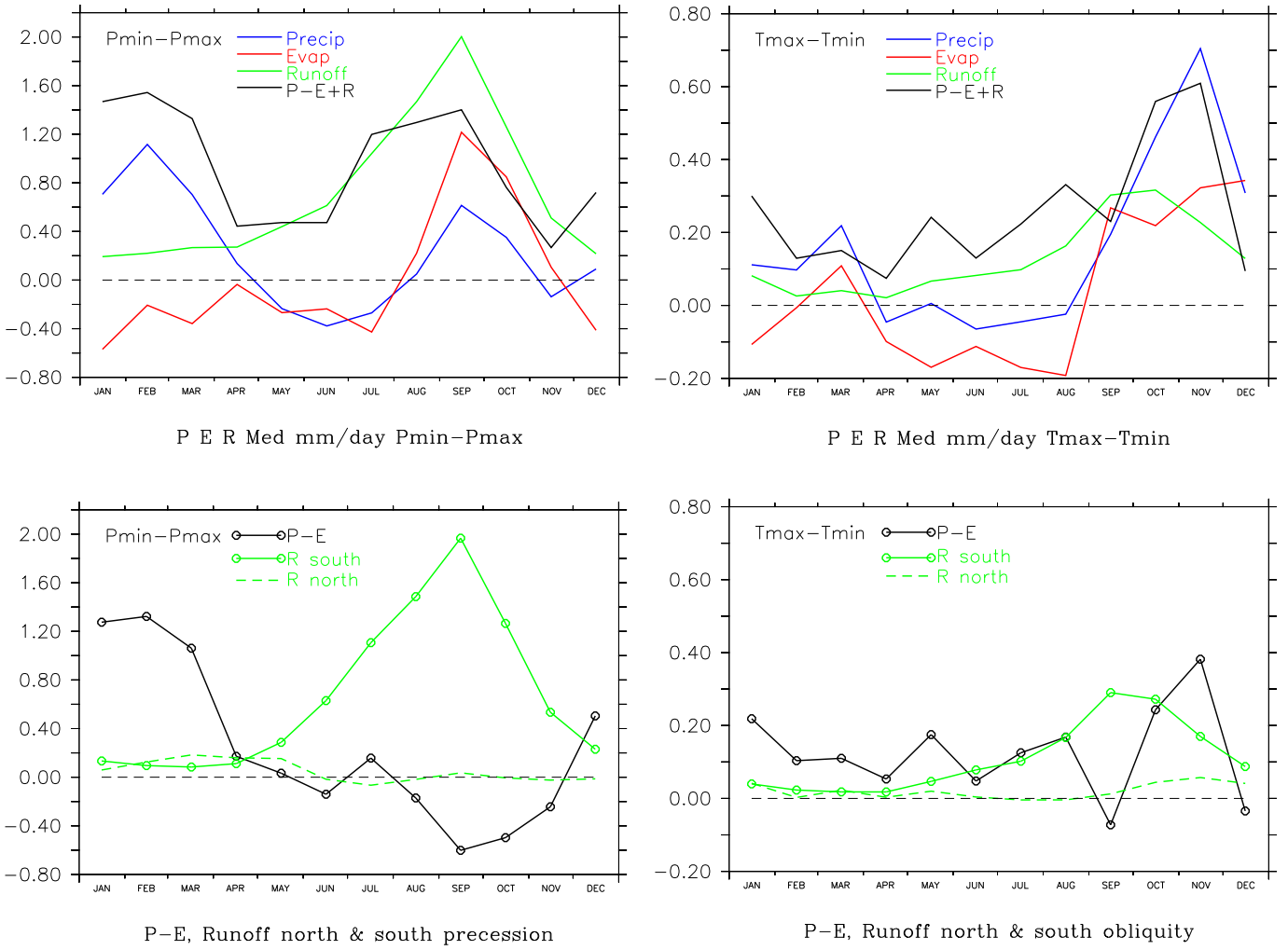

Fig. 4. Precipitation, evaporation, runoff, P-E + R and P-E over the Mediterranean Sea, differences between experiments Pmin and Pmax (left), Tmax and Tmin (right) in mm/day. Note that the scales on the y-axes of a,c are different than those of b,d. Only gridpoints over ocean are taken into account. Runoff from the Chad basin is subtracted for this figure; runoff from the south is mainly from the Nile River.

higher air temperatures, resulting in lower relative humidity as well as a smaller air-sea temperature difference (Fig. 9(a) and (c)). The latter gives rise to more stable conditions in the (lower) atmosphere, resulting in less precipitation. Precipitation is reduced even more over southern Europe in Pmin compared to Pmax (Fig. 6(a)), explaining the (small) decrease in summer river runoff from the north. At the same time precipitation over northern Africa and the Middle-East is increased in both the Pmin and Tmax experiments. Overall, net precipitation (P-E) is slightly reduced during summer for Pmin (Fig. 4(c)). For Tmax, evaporation is reduced more than precipitation, resulting in a small increase in summer P-E (Fig. 4(d)). Over the eastern Mediterranean, reduced evaporation (Figs. 6(c), 10(c)) leads to increased P-E for both Pmin and Tmax (not shown).

3.4. Winter

The increase in (net) precipitation over the basin in the Pmin and Tmax experiments occurs mostly in the winter months (Fig. 4). Precipitation increases are largest over the eastern Mediterranean, specifically over the Ionian and Levantine Seas (Figs. 6(b), 10(b)), as well as near the coasts of Spain and Morocco. Winter precipitation increases have previously been attributed to increased storm track activity over the Mediterranean (e.g. Kutzbach et al., 2013). Here we find a reduced equator-to-pole winter temperature gradient (not shown), related to a reduced equator-to-pole insolation gradient (especially for precession), and reduced storm track activity over the North Atlantic in Pmin and Tmax. Over the Mediterranean area the storm track activity is also reduced, as indicated by the standard deviation of the 500 hPa geopotential height (Kaspar et al., 2007) (Fig. 8(a) and (b)). Lower relative vorticity over the Mediterranean in Pmin further indicates reduced storm track activity (not shown). In Tmax there is a slight increase in storm activity west of Spain/Morocco (Fig. 8(b)), where winter precipitation is increased (Fig. 10(b)).

Using variance of sea level pressure (SLP) instead of 500 hPa geopotential height as a measure for storm track activity yields similar results, except that SLP variance is increased over western Spain/Morocco in Pmin (Fig. 8(c)). Probably more shallow storms occur here, explaining the precipitation increase (Fig. 6(b)). In Tmax the increased storm tracks over western Spain/Morocco are less clear from SLP (Fig. 8(d)) during the winter half year, but during November–December (when precipitation changes for obliquity are largest) the increased storm track activity over Spain/Morocco appears in both the Z500 and SLP analyses.

Moreover, there is a clear contrast in precipitation changes over land and sea, which likely would not be the case if precipitation

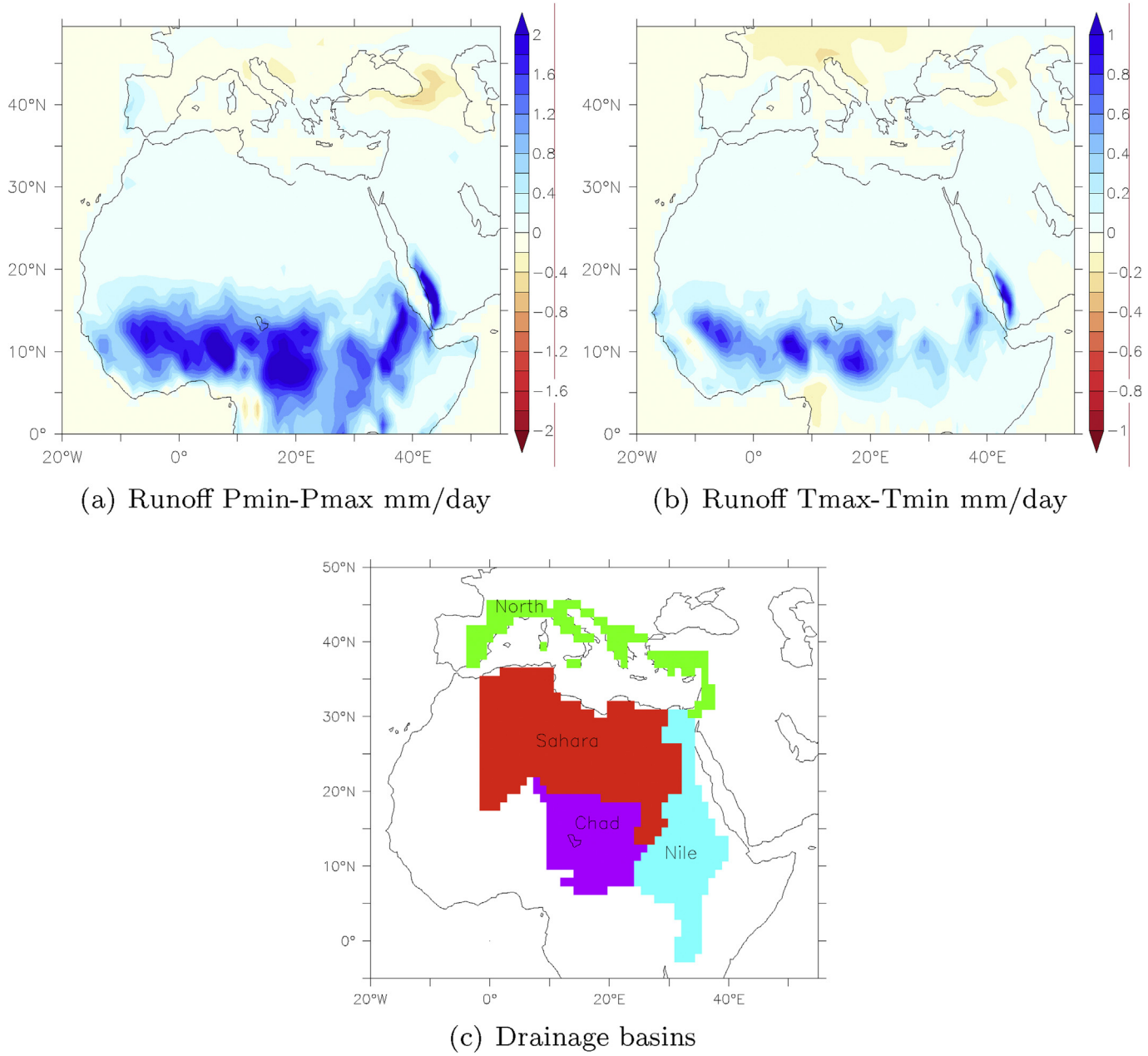

Fig. 5. Annual mean runoff change over land for precession (a) and obliquity (b). Note the smaller colour scale in (b) compared to (a). Figure (c) shows the four drainage basins that drain into the Mediterranean in EC-Earth. (For interpretation of the references to colour in this figure legend, the reader is referred to the web version of this article.)

changes were mainly due to increased storm track activity. An alternative mechanism explaining the winter precipitation increase is a stronger contrast in sea surface and air temperatures (Fig. 9(b) and (d)). Both SST and surface air temperatures are reduced in winter due to reduced insolation, but surface air temperature decreases more strongly than SST. The latter lags the insolation forcing due to a strong heat capacity, increasing the sea-air temperature contrast and leading to more unstable conditions. Indeed most of the precipitation increase in the winter over the basin is from convective rain, not large scale rain, occurring over areas where the temperature contrast is strengthened most, see Fig. 10. Convective rain also explains the majority of the basin-averaged precipitation changes per month (not shown, see Fig. 4(a) and (b)), with convective precipitation increase peaking in February for precession and in November for obliquity. Only the precipitation increase near the coast of Spain/Morocco is partly large scale, in agreement with increased SLP variance over this area.

For Pmin, net precipitation is increased due to increased precipitation as well as reduced evaporation, while for Tmax increased evaporation counteracts the precipitation increase, especially in autumn/early winter (Fig. 4(a) and (b)).

3.5. Possible effects of changes in the freshwater budget on deep water formation

Here we briefly show changes in surface salinity and mixed layer depth, in order to describe possible effects of the above-mentioned precession- and obliquity-induced changes in the surface freshwater budget on ocean circulation. The general hypothesis is that at times of increased NH summer insolation, increased river runoff

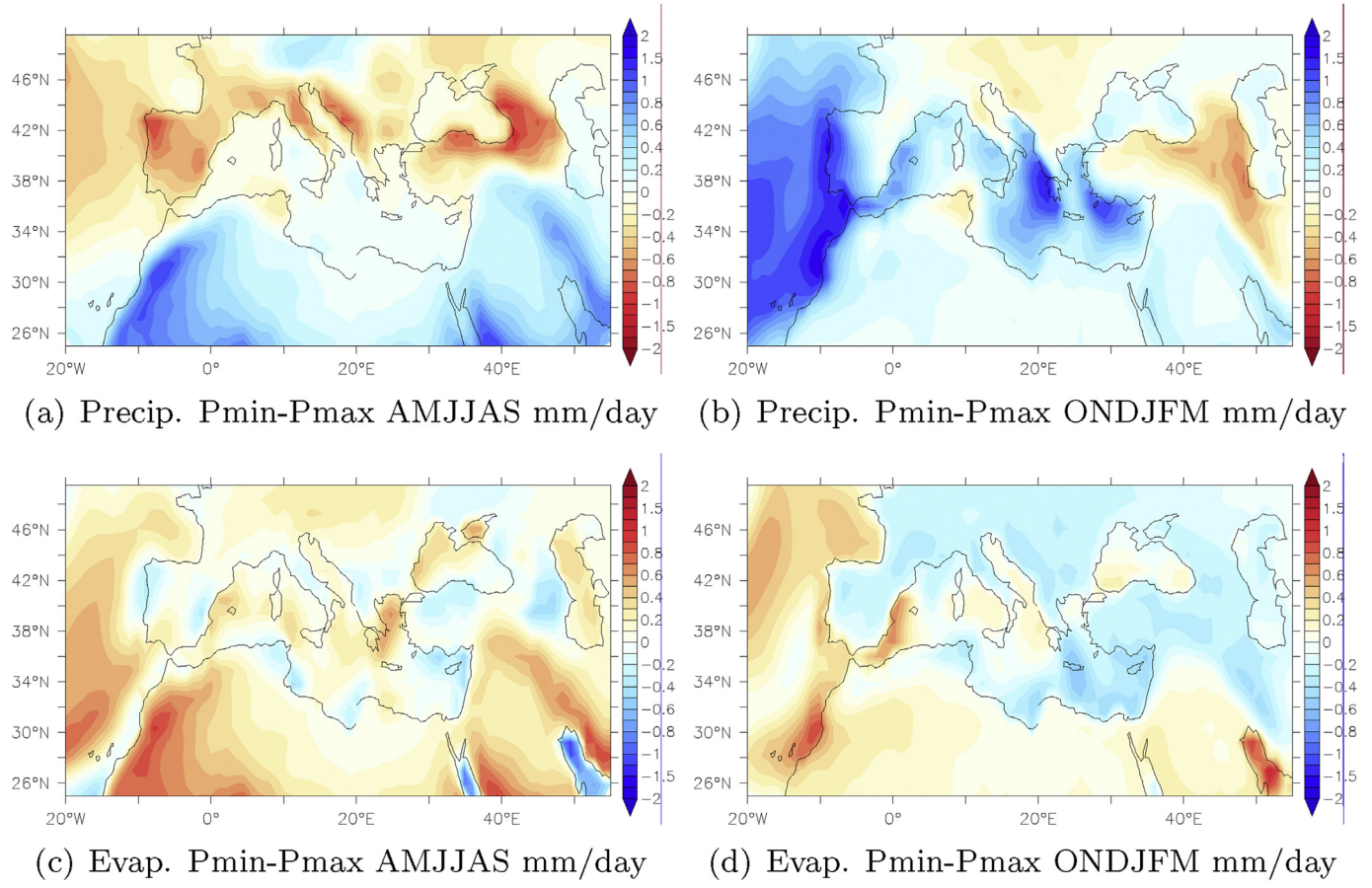

Fig. 6. Precipitation and evaporation changes Pmin − Pmax in mm/day per half year (AMJJAS is April–September, ONDJFM is October–March). Positive values indicate increased precipitation or increased evaporation, blue colours indicate an increase in freshwater flux towards the surface. (For interpretation of the references to colour in this figure legend, the reader is referred to the web version of this article.)

from North Africa into the Mediterranean reduces the surface salinity, resulting in a more stable stratification. With a more stable stratification there is a reduction (or even elimination) of intermediate and deep water formation, and therefore less supply of oxygen to the deep ocean, favouring the development of sapropels (e.g. Rossignol-Strick, 1985; Rohling, 1994; Rohling et al., 2004; Marino et al., 2007; Rohling et al., 2009).

In the pre-industrial experiment, the mixed layer is deepest in winter in the southern Aegean Sea/northern Levantine (reaching ~400 m) and in the Gulf of Lion (reaching over 500 m, not shown), i.e. locations of intermediate and deep water formation, in line with the climatology of D'Ortenzio et al. (2005). The model does not reproduce a deep mixed layer in the Adriatic Sea; likely the model cannot simulate the small-scale (i.e. sub-grid) deep water ventilation that is known to occur in this area.

In the previous sections we found an increased freshwater budget (P-E + R) in the Pmin and Tmax experiments, due to enhanced runoff and winter precipitation over the basin. Further freshening occurs through increased runoff from the Chad basin towards the Mediterranean (Table 2, Section 2). This freshening results in reduced surface salinity, as shown in Fig. 11(a) and (b). These figures show the annual surface salinity changes (the surface layer in NEMO is 10 m thick); the pattern of salinity changes hardly varies per season (not shown). In Pmin, surface salinity is lower over the whole basin, mostly near the entrance points of runoff from the Nile river and the Chad basin (the Nile delta and Gulf of Sirte, Fig. 11(a)). In Tmax, salinity is decreased in the south-eastern part of the basin as well, while the western basin experiences little change (Fig. 11(b)). The strong salinity increase in the Black Sea in Tmax could be related to increased winter evaporation (Fig. 10(d)) and/or diminished Danube river runoff due to reduced precipitation over Middle Europe (Fig. 10(a) and (b)).

The freshening at the surface reduces the formation of intermediate and deep water, as exemplified by a reduction in the mixed layer depth in the Pmin and Tmax experiments (Fig. 11(c) and (d)). These figures show the mixed layer depth changes in February, which is when the mixed layer is deepest and most intermediate and deep water is formed. For precession, the largest changes occur at the area of intermediate water formation in the southern Aegean Sea/northern Levantine and in the Gulf of Lion, a location of deep water formation. In the latter region the decrease in surface salinity is not as large as in the east, but a reduction in the northwesterly winds over this area in winter (not shown) further helps to reduce vertical mixing. In Tmax, the mixed layer depth in the Gulf of Lion is increased compared to Tmin, while a shallower mixed depth occurs in the south-east where surface salinity is decreased.

4. Discussion

In this study we have investigated orbitally forced changes in (net) precipitation and runoff over the Mediterranean. It is the first study of this subject to use a high resolution fully coupled GCM applying separate precession and obliquity forcing. Here we discuss the implications of our results for changes in summer runoff and precipitation, winter precipitation and deep water formation compared to proxy data as well as other model studies.

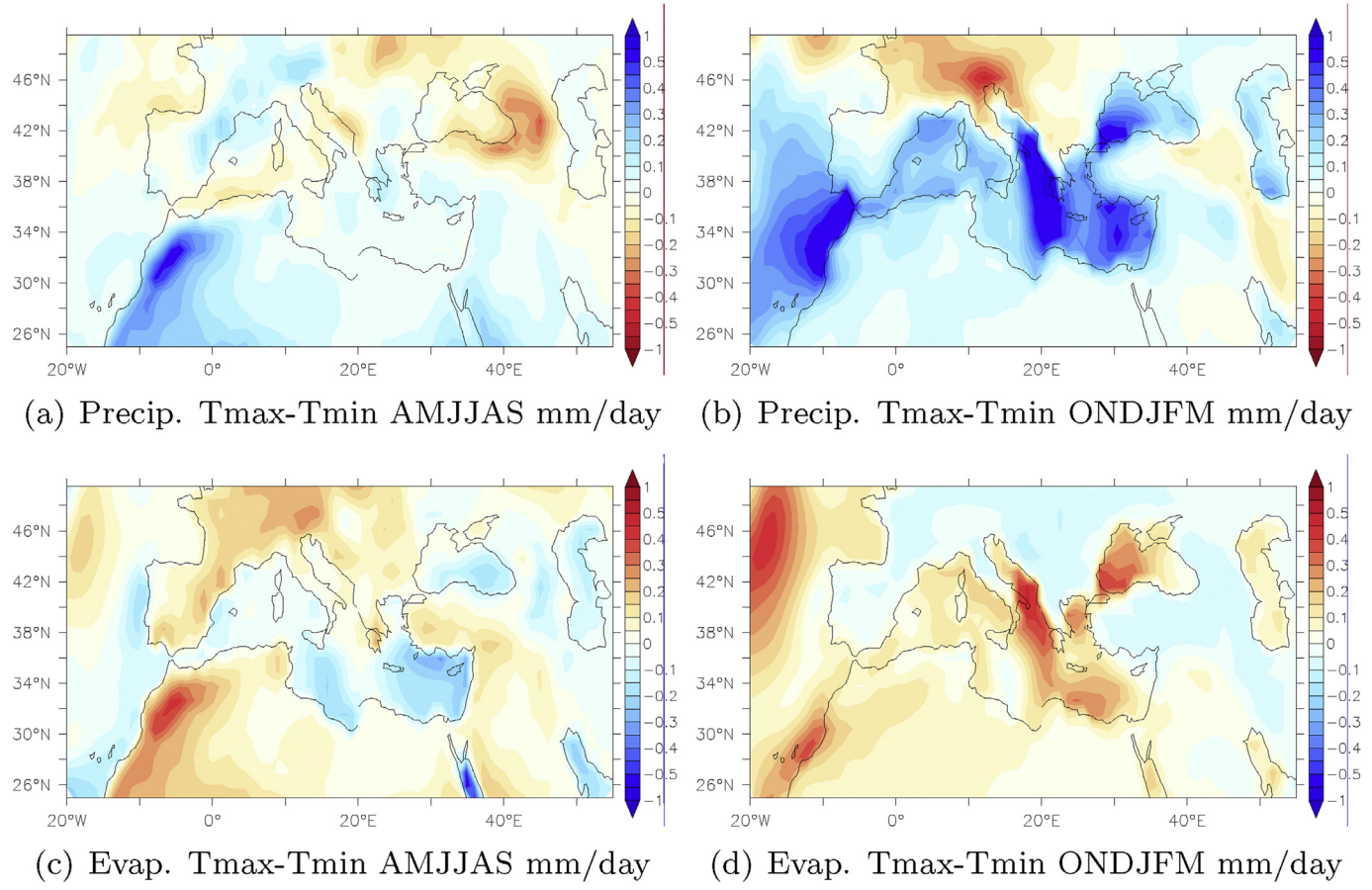

Fig. 7. Precipitation and evaporation changes Tmax − Tmin in mm/day per half year (AMJJAS is April–September, ONDJFM is October–March). Positive values indicate increased precipitation or increased evaporation, blue colours indicate an increase in freshwater flux towards the surface. (For interpretation of the references to colour in this figure legend, the reader is referred to the web version of this article.)

4.1. Summer (monsoon) runoff and precipitation

The strengthening of the North African monsoon in the Pmin and Tmax experiments, forcing enhanced runoff from the south into the Mediterranean during summer and autumn, is in line with previous studies (Rohling et al., 2009; Kutzbach et al., 2013; Bosmans et al., 2015, and references therein). Nile river runoff may also be influenced by the Indian monsoon (e.g. Hennekam et al., 2014; Weldeab et al., 2014), which is strengthened at times of increased summer insolation as well (e.g. Bosmans et al., 2012), but a discussion of the relative roles of the African and Indian monsoon is beyond the scope of this study. Besides increased Nile river runoff, fresh water also enters the Mediterranean further west, along the coast of present-day Libya. Although the main source of this runoff in our experiments, the Chad basin, is not realistic for geologically-recent periods, there is ample evidence that monsoon runoff did enter the Mediterranean in this area at times of high summer insolation. Satellite images show now-buried fossil river systems in the Sahara, which may have reached from the mountains in the Sahara, such as the Tibesti mountains, to the Mediterranean coast (Paillou et al., 2009, 2012). Lakes existed in the now-arid Sahara, such as in the Libyan Fezzan region (e.g. Gaven et al., 1981). Such rivers and lakes provided humid corridors towards the Mediterranean during astronomically forced "Green Sahara Periods", such as the early Holocene and especially the Eemian, when the North African monsoon crossed the Saharan watershed at ~21° N (e.g. Pachur and Braun, 1980; Hoelzmann et al., 1998; Rohling et al., 2002; Osborne et al., 2008; Drake et al., 2011; Larrasoaña et al., 2013; Rohling et al., 2015). Further evidence of monsoon runoff reaching the Mediterranean along the wider North African margin stems from isotope analysis. Osborne et al. (2008, 2010) show a strong neodymium (Nd) isotope signal especially in the Ionian Sea, suggesting runoff from North Africa at times of enhanced summer insolation from a source west of the Nile river. Such a source would also explain exceptionally low oxygen isotope values, likely originating from heavy monsoon precipitation, between Crete and Libya (e.g. Rohling et al., 2002, 2004; Emeis et al., 2003, 2009). Coulthard et al. (2013) showed that humid corridors along the wider North African margin were very likely during the last interglacial (Eemian), using paleohydrological and hydraulic modelling. In EC-Earth the monsoon does not reach sufficiently northward to provide runoff north of 21° N (see Fig. 5, Bosmans et al., 2015), not even during minimum precession. This is likely related to the lack of dynamic vegetation; increased monsoon precipitation would lead to a wetter and greener Sahara, and therefore an additional strengthening and northward extension of the monsoon through a lowered albedo (e.g. Brovkin et al., 1998; Ganopolski et al., 1998; Claussen et al., 1999; Levis et al., 2004; Herold and Lohmann, 2009; Timm et al., 2010) and/or increased evaporation and transpiration from the larger lakes and wetlands Krinner et al. (2012) or from vegetated areas Rachmayani et al. (2015). Despite the idealized set-up of our experiment, using present-day vegetation as a boundary condition, our results provide an explanation for an enhanced freshwater flux into the

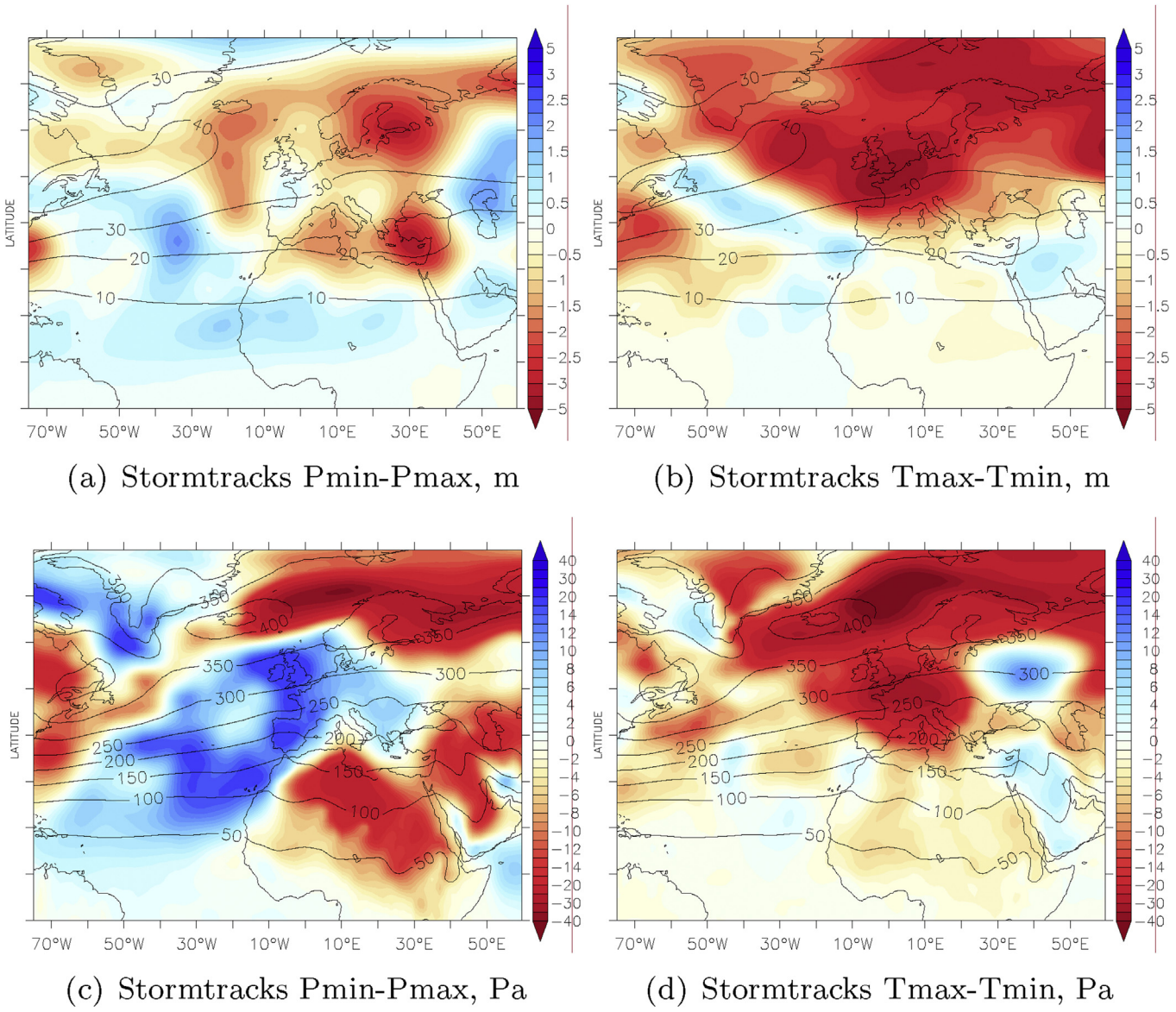

Fig. 8. Storm track activity changes based on the standard deviation of 2.5–8 day filtered 500 hPa geopotential height for winter (a,b in meter) (ONDJFM). Also shown is storm track activity based on the variance of 2.5–8 day filtered sea level pressure for ONDJFM (c,d in Pa).

Mediterranean Sea that could be valid for many precession minima, given the close coincidence between sapropels and "Green Sahara Periods", i.e. precession minima, throughout the last 8Myr (Larrasoaña et al., 2013).

Over the Mediterranean Sea itself precipitation is slightly decreased during summer, as opposed to the inferences of Rossignol-Strick (1987); Rohling and Hilgen (1991); Rohling (1994). More recently, increased precipitation at times of high insolation seasonality has been attributed to winter precipitation instead of summer precipitation (Tzedakis, 2007, 2009; Kutzbach et al., 2013; Rohling et al., 2015, and references therein), which is corroborated by our study. In the Middle East, summer and winter precipitation is increased in our minimum precession and maximum obliquity experiments, which could explain why isotopic evidence from Israeli speleothems suggest increased precipitation at times of summer aridity over the Mediterranean (Bar-Matthews et al., 2000; Tzedakis, 2007). However, there is some debate whether the Israeli cave records reflect precipitation changes or changes in precipitation source (e.g. Bar-Matthews et al., 2003; Kolodny et al., 2005; Roberts et al., 2008; Almogi-Labin et al., 2009; Grant et al., 2012).

4.2. Winter precipitation

We find that changes in winter precipitation over the Mediterranean basin can be of the same order of magnitude as changes in (monsoon) runoff, playing an important role in the freshwater budget changes, especially for obliquity. The simultaneous occurrence of increased summer monsoon runoff and winter precipitation was also pointed out in the model studies of Meijer and Tuenter (2007) and Kutzbach et al. (2013). Meijer and Tuenter (2007) indicate the importance of enhanced winter river runoff from the north during minimum precession, but in our experiments runoff from the north shows very little change. Furthermore, isotope analysis shows no additional runoff from the north and instead suggest a monsoonal freshwater source in the Aegean and Ionian Seas (Osborne et al., 2010). Rohling et al. (2015) state that

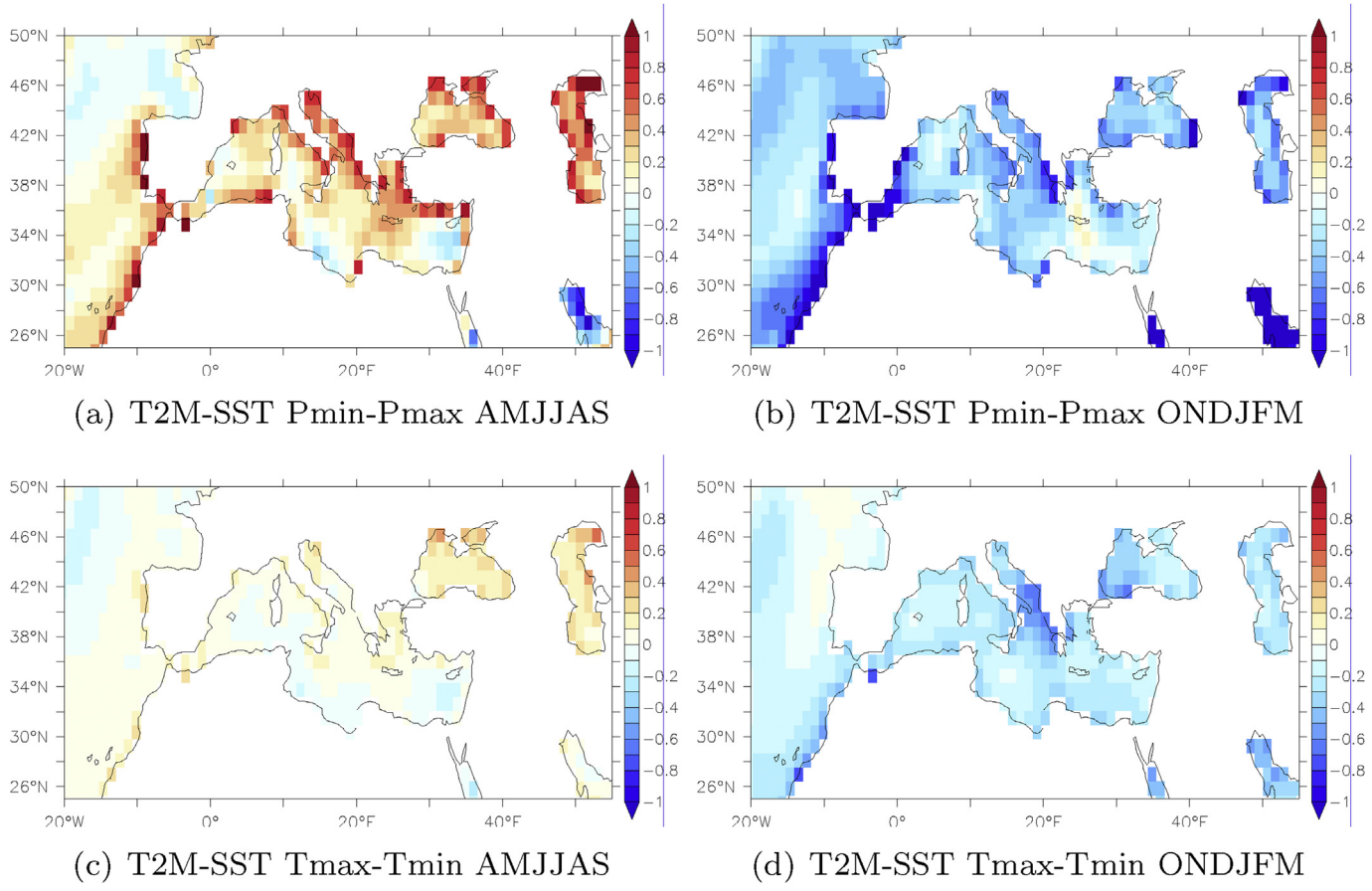

Fig. 9. Differences in the T2M-SST difference in degrees. T2M is generally lower than SST, so negative values indicate a stronger difference, i.e. more unstable conditions.

excess winter precipitation over the borderlands was predominately sourced from the Mediterranean Sea itself. Kutzbach et al. (2013) find increased winter precipitation over both the Mediterranean Sea as well as its borderlands during minimum precession, linked to increased Mediterranean storm track activity. In contrast to Kutzbach et al. (2013) we identify winter precipitation increases over certain locations over the Sea itself, not over the whole Mediterranean area, as well as weaker storm track activity over both the Mediterranean and the North–Atlantic in both Pmin and Tmax, presumably due to weaker meridional temperature gradients. There is as of yet no consensus on orbitally forced changes in the storm tracks: Kaspar et al. (2007) find increased North–Atlantic storm tracks and weakened Mediterranean storm tracks during the Eemian (a time of minimum precession), Hall and Valdes (1997) show a slightly stronger North–Atlantic storm track during the Mid-Holocene, whereas Brayshaw et al. (2011) state that a southward shift and therefore reduced North–Atlantic and an increased Mediterranean storm tracks occur during the Early Holocene. In precession experiments similar to ours, Kutzbach et al. (2013) find increased Mediterranean storm tracks. These different findings may be related to differences in model parametrisations and resolution. Kutzbach et al. (2013) base their findings on a low resolution model (~3.75°), and note that in higher-resolution Eemian and Mid-Holocene experiments with the same model the changes in Mediterranean precipitation and surface pressure are similar, but not completely identical to changes in the extreme precession experiments. Our state-of-the-art high-resolution model indicates that changes in storm track activity do not explain the changes in Mediterranean winter precipitation; instead we attribute increased winter precipitation to an increased temperature difference between the sea surface and overlaying air, causing more unstable conditions and more locally generated convective precipitation. Moreover, the patterns of difference in winter precipitation are very similar to the patterns in observed and modelled winter precipitation (Figs. 2, 6 and 7), which is mostly related to evaporation from the basin itself (see Section 3.1). The role of external triggers of cyclones in the Mediterranean, or the reason for the reduced storm track activity, are subjects for further study. For instance the use of a higher atmospheric resolution than our ~100 km to capture orography and small-scale processes even better, could shed more light on the specific role of convective precipitation and the complex interaction of Mediterranean cyclogenesis and air flowing in from the Atlantic and Eurasia.

In literature, the assumption that increased winter precipitation is caused by increased storm track activity at times of enhanced insolation seasonality has also risen from the similarity between sapropel sequences in the Mediterranean and sedimentary sequences in western Spain and Morocco (Sierro et al., 2000; van der Laan et al., 2012). Both regions were wetter at times of enhanced insolation seasonality; increased storm track activity would provide more moisture to both regions. Here we show that the two regions might indeed receive more moisture simultaneously but for different reasons; at least part of the winter precipitation change increase over western Spain and Morocco may be related to storm tracks, while precipitation change over the Mediterranean basin is driven by locally driven convective precipitation. Furthermore, monsoon precipitation may reach Morocco in summer (Bosmans et al., 2015).

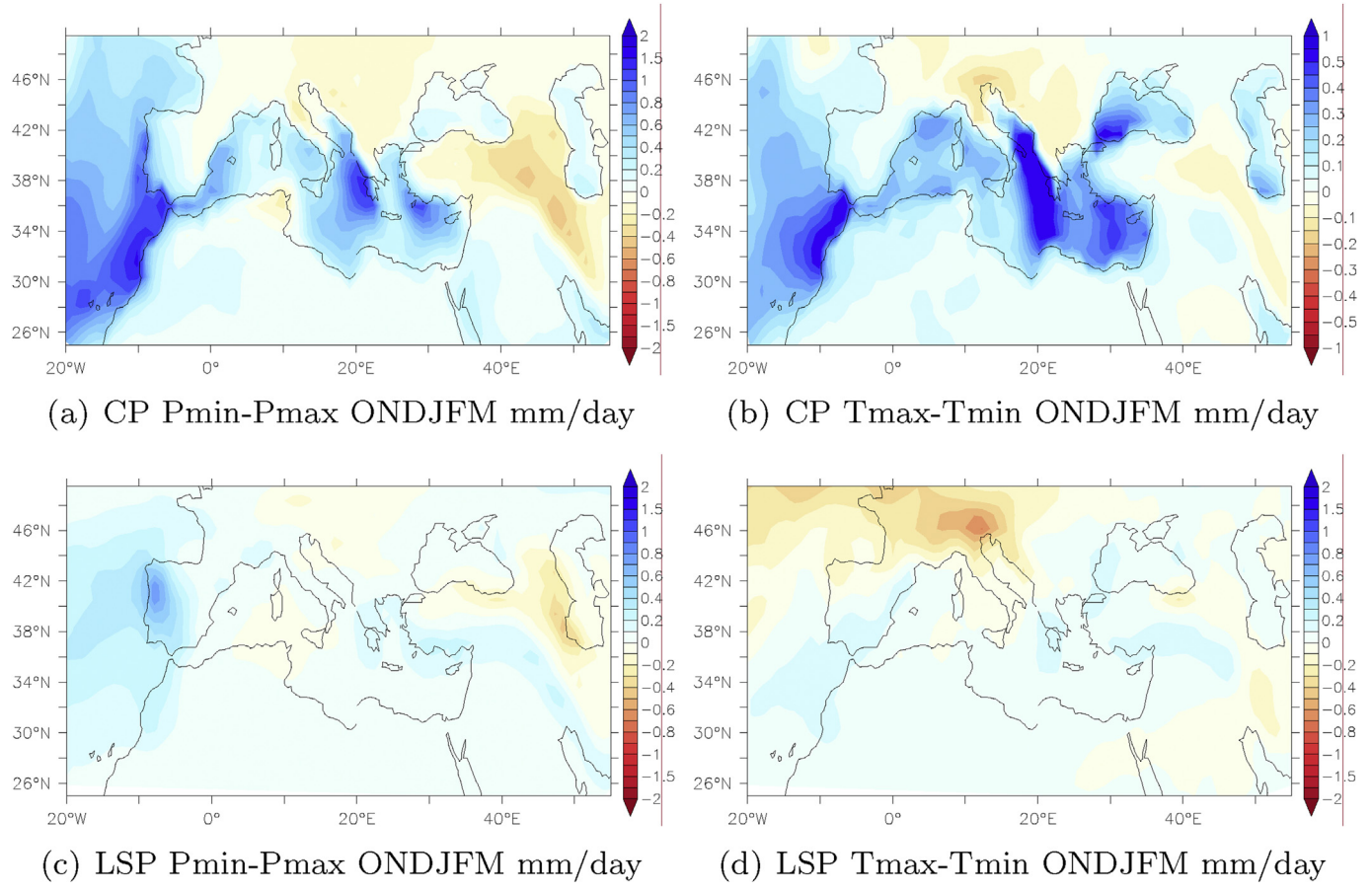

Fig. 10. Changes in winter (ONDJFM) convective precipitation (CP, top) and large scale precipitation (LSP, bottom) for precession (left) and obliquity (right) in mm/day. Note the different scales used for precession and obliquity.

4.3. Mediterranean Sea deepwater formation

Both the increased winter precipitation and summer (monsoon) runoff result in a freshening of the Mediterranean in all months in both the Pmin and Tmax experiments. The oceanic response to the increased freshwater flux is a reduction in salinity and mixed layer depth, indicating stronger stratification and less intermediate and deep water formation. Such changes are in line with the formation of sapropels at times of enhanced insolation seasonality (e.g. Rossignol-Strick, 1985; Rohling et al., 2015). The modelled (surface) salinity changes, consisting especially of reduced salinity where freshwater from North Africa enters the Mediterranean, also indicate a strong change in the east-west salinity gradient (Emeis et al., 2003). We cannot determine whether summer runoff or winter precipitation over the basin is the dominant forcing of changes in stratification and deep water formation. Winter precipitation may be more important for deep water formation, as the latter occurs in the winter months and winter precipitation changes are strong over the northern Levantine and the Adriatic/Ionean sea, regions of intermediate- and deepwater formation. Further investigation with a regional ocean model could shed more light on the dominant mechanism of changes in salinity and stratification. This was previously endeavoured by Meijer and Tuenter (2007). However, the freshwater forcing in their study was derived from an intermediate complexity model (EC-Bilt), which showed a different response to the same orbital forcings as EC-Earth (Bosmans et al., 2015), and their ocean model did not simulate the full circulation. Moreover, the salinity and mixed layer depth changes we found in this study could have an effect on the exchange of water at the Strait of Gibraltar, with for instance less saline water entering the Atlantic at times of enhanced insolation seasonality.

Additionally, the oceanic response in EC-Earth includes a response to changes in Chad runoff, which could be excluded in a future sensitivity study in order to investigate the oceanic response to precession and obliquity under more realistic (geologically recent) boundary conditions. Further back in time, during the late Miocene, Chad runoff may have entered the Mediterranean (Gladstone et al., 2007; Griffin, 2011). Our study shows that Chad runoff could play a large role in the Mediterranean freshwater budget and therefore the ocean circulation. However the Mediterranean topography was quite different during the Miocene, so the role of Chad runoff at that time needs to be investigated using Miocene boundary conditions. We note that major river runoff did occur through Libya at times of enhanced summer insolation such as the early Holocene and especially the Eemian (see Section 4.1), but this runoff likely originated from monsoon precipitation crossing the Saharan watershed at 21° N during peak summer, not from lake Chad.

5. Conclusions

Based on our EC-Earth experiments of the separate precession and obliquity signals, we conclude that orbitally forced changes in the Mediterranean freshwater budget are mainly driven by (monsoonal) river runoff from the south and winter precipitation over the basin itself. River runoff from the south, related to the

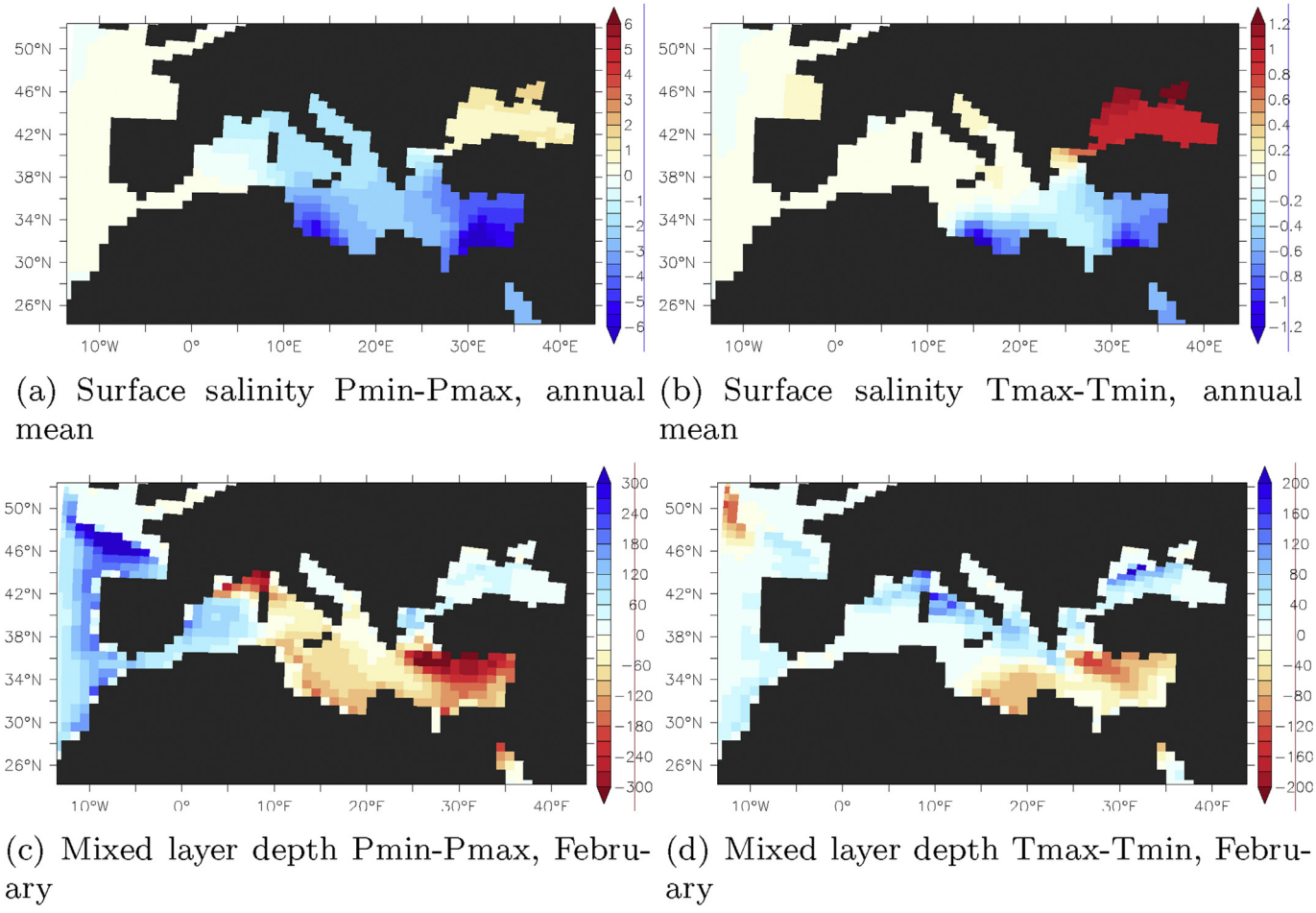

(a) Surface salinity Pmin-Pmax, annual mean

(b) Surface salinity Tmax-Tmin, annual mean

(c) Mixed layer depth Pmin-Pmax, February

(d) Mixed layer depth Tmax-Tmin, February

Fig. 11. Surface salinity changes (a, b, annual, in g/kg) and changes in mixed layer depth (where density exceeds the surface density by 1%) (c,d, February). For mixed layer depth, negative values (red colours) indicate shallower depth. Note the salinity changes in the Gulf of Sirte due to increased runoff from the Chad basin, which was ignored in the freshwater flux discussed in this study. The colour key is larger for the precession than for the obliquity figures. (For interpretation of the references to colour in this figure legend, the reader is referred to the web version of this article.)

Table 2
Annual mean values and changes in the components of the freshwater budget in mm/day averaged over the Mediterranean Sea (only gridpoints over the sea are taken into account). Both precipitation ("gain") and evaporation ("loss") are listed as positive values. Runoff from the south is from the Nile and Sahara basins, the runoff (R) and net loss (E-P-R) excludes Chad runoff. The last column shows the % change w.r.t. the pre-industrial.

	Pre-ind [mm/day]	Pmin [mm/day]	Pmax [mm/day]	Pmin-Pmax [mm/day]	(Pmin-Pmax)/PI %
Evaporation (E)	3.37	3.31	3.32	−0.01	−0.3%
Precipitation (P)	1.54	1.59	1.37	0.22	15%
River runoff (R)	0.44	1.02	0.31	0.71	160%
Id. from north	0.30	0.31	0.27	0.04	15%
Id. from south	0.14	0.70	0.04	0.66	474%
Id. from Chad	0.06	0.95	0.01	0.94	1591%
Net loss (E-P-R)	1.38	0.70	1.65	−0.95	−72%
Net loss (with Chad)	1.33	−0.25	1.63	−1.89	−142%
Net inflow Gibraltar	1.17	−0.33	1.44	−1.77	−150%
Net inflow Black Sea	0.20	0.12	0.24	−0.12	−60%
	Pre-ind [mm/day]	Tmax [mm/day]	Tmin [mm/day]	Tmax-Tmin [mm/day]	Tmax-Tmin/PI %
Evaporation (E)	3.37	3.38	3.35	0.03	1.0%
Precipitation (P)	1.54	1.63	1.47	0.16	10%
River runoff (R)	0.44	0.60	0.47	0.13	29%
Id. from north	0.30	0.32	0.30	0.02	7%
Id. from south	0.14	0.28	0.17	0.11	79%
Id. from Chad	0.06	0.34	0.10	0.24	402%
Net loss (E-P-R)	1.38	1.16	1.41	−0.25	−19%
Net loss (with Chad)	1.33	0.82	1.31	−0.49	−37%
Net inflow Gibraltar	1.17	0.77	1.21	−0.45	−38%
Net inflow Black Sea	0.20	0.12	0.16	−0.04	−20%

strength of the North African monsoon, dominates the freshwater budget changes for precession. Changes in winter precipitation, which we relate to a stronger air-sea temperature difference and locally induced convective precipitation instead of storm track activity, dominate freshwater budget changes for obliquity. The freshening in the minimum precession and maximum obliquity experiments have a strong effect on Mediterranean surface salinity and mixed layer depth, and may therefore lead to stratification and consequently sapropel formation.

Acknowledgements

We thank Dr. Hylke de Vries and Dr. Rein Haarsma (Royal Netherlands Meteorological Institute, KNMI) for help with diagnosing storm tracks and discussing the outcomes. Computing time was provided by KNMI and the European Centre for Medium-range Weather Forecasts (ECMWF). This research was part of Dr. Bosmans' PhD project, funded by a "Focus en Massa" grant from Utrecht University, and was carried out at the department of Earth Sciences and KNMI.

References

Adloff, F., Mikolajewicz, U., Kucera, M., Grimm, R., Maier-Reimer, E., Schmiedl, G., Emeis, K.-C., 2011. Upper ocean climate of the Eastern Mediterranean sea during the holocene insolation maximum – a model study. Clim. Past 7, 1103–1122. http://dx.doi.org/10.5194/cp-7-1103-2011.

Almogi-Labin, A., Bar-Matthews, M., Shriki, D., Kolosovsky, E., Paterne, M., Schilman, B., Ayalon, A., Aizenshtat, Z., Matthews, A., 2009. Climatic variability during the last 90ka of the southern and northern Levantine Basin as evident from marine records and speleothems. Quat. Sci. Rev. 28, 2882–2896.

Bar-Matthews, M., Ayalon, A., Kaufman, A., 2000. Timing and hydrological conditions of Sapropel events in the Eastern Mediterranean, as evident from speleothems, Soreq cave, Israel. Chem. Geol. 169, 145–156.

Bar-Matthews, M., Ayalon, A., Gilmour, M., Matthews, A., Hawkesworth, C.J., 2003. Sea–land oxygen isotopic relationships from planktonic foraminifera and speleothems in the Eastern Mediterranean region and their implication for paleorainfall during interglacial intervals. Geochim. Cosmochim. Acta 67, 3181–3199.

Bengtsson, L., Hodges, K.I., Roeckner, E., 2006. Storm tracks and climate change. J. Clim. 19, 3518–3543.

Bosmans, J.H.C., Drijfhout, S.S., Tuenter, E., Lourens, L.J., Hilgen, F.J., Weber, S.L., 2012. Monsoonal response to mid-holocene orbital forcing in a high resolution GCM. Clim. Past 8, 723–740. http://dx.doi.org/10.5194/cp-8-723-2012.

Bosmans, J.H.C., Drijfhout, S.S., Tuenter, E., Hilgen, F.J., Lourens, L.J., 2015. Response of the North African summer monsoon to precession and obliquity forcings in the EC-Earth GCM. Clim. Dyn. 44, 279–297. http://dx.doi.org/10.1007/s00382-014-2260-z.

Brayshaw, D.J., Rambeau, C.M.C., Smith, S.J., 2011. Changes in Mediterranean climate during the Holocene: Insight from global and regional climate modelling. Holocene 21, 15–31. http://dx.doi.org/10.1177/0959683610377528.

Brovkin, V., Claussen, M., Petoukhov, V., Ganopolski, A., 1998. On the stability of the atmosphere-vegetation system in the Sahara/Sahel region. J. Geophys. Res. 103, 31 613–31 624.

Claussen, M., Kubatzki, C., Brovkin, V., Ganopolski, A., 1999. Simulation of an abrupt change in Saharan vegetation in the mid-Holocene. Geophys. Res. Lett. 26, 2037–2040.

Coulthard, T.J., Ramirez, J.A., Barton, N., Rogerson, M., Brücher, T., 2013. Were rivers flowing across the sahara during the last interglacial? Implications for human migration through Africa. PLoS One 8, e74 834.

Criado-Aldeanueva, F., Soto-Navarro, F., Garcia-Lafuente, J., 2012. Seasonal and interannual variability of surface heat and freshwater fluxes in the Mediterranean Sea: budgets and exchange through the Strait of Gibraltar. Int. J. Climatol. 32, 286–302. http://dx.doi.org/10.1002/joc.2268.

Dee, D.P., Uppala, S.M., Simmons, A.J., Berrisford, P., Poli, P., Kobayashi, S., Andrae, U., Balmaseda, M.A., Balsamo, G., Bauer, P., Bechtold, P., Beljaars, A.C.M., van de Berg, L., Bidlot, J., Bormann, N., Delsol, C., Dragani, R., Fuentes, M., Geer, A.J., Haimberger, L., Healy, S.B., Hersbach, H., Hlm, E.V., Isaksen, L., Kllberg, P., Khler, M., Matricardi, M., McNally, A.P., Monge-Sanz, B.M., Morcrette, J.-J., Park, B.-K., Peubey, C., de Rosnay, P., Tavolato, C., Thpaut, J.-N., Vitart, F., 2011. The ERA-Interim reanalysis: configuration and performance of the data assimilation system. Q. J. R. Meteorol. Soc. 137, 553–597. http://dx.doi.org/10.1002/qj.828.

D'Ortenzio, F., Iudicone, D., de Boyer Montegut, C., Testor, P., Antoine, D., Marullo, S., Santoleri, R., Madec, G., 2005. Seasonal variability of the mixed layer depth in the Mediterranean Sea as derived from in situ profiles. Geophys. Res. Lett. 32 http://dx.doi.org/10.1029/2005GL022463.

Drake, N.A., Blench, R.M., Armitage, S.J., Bristow, C.S., White, K.H., 2011. Ancient watercourses and biogeography of the Sahara explain the peopling of the desert. Proc. Natl. Acad. Sci. 108, 458–462. http://dx.doi.org/10.1073/pnas.1012231108.

Emeis, K.-C., Schulz, H., Struck, U., Rossignol-Strick, M., Erlenkeuser, H., Howell, M., Kroon, D., Mackensen, A., Ishizuka, S., Oba, T., et al., 2003. Eastern Mediterranean surface water temperatures and δ^{18} O composition during deposition of sapropels in the late Quaternary. Paleoceanography 18.

Ganopolski, A., Kubatzki, C., Claussen, M., Brovkin, V., Petoukhov, V., 1998. The influence of vegetation-atmosphere-ocean interaction on climate during the mid-Holocene. Science 280, 1916–1919.

Gaven, C., Hillaire-Marcel, C., Petit-Maire, N., 1981. A Pleistocene lacustrine episode in southeastern Libya. Nature 290, 131–133.

Gladstone, R., Flecker, R., Valdes, P., Lunt, D., Marwick, P., 2007. The Mediterranean hydrologic budget from a Late Miocene global climate simulation. Palaeogeogr. Palaeoclimatol. Palaeoecol. 251, 254–267.

Grant, K., Rohling, E., Bar-Matthews, M., Ayalon, A., Medina-Elizalde, M., Ramsey, C.B., Satow, C., Roberts, A., 2012. Rapid coupling between ice volume and polar temperature over the past 150,000 [thinsp] years. Nature 491, 744–747.

Griffin, D.L., 2011. The late Neogene Sahabi rivers of the Sahara and the hamadas of the eastern LibyaChad border area. Palaeogeogr. Palaeoclimatol. Palaeoecol. 309, 176–185.

Hall, N.M.J., Valdes, P.J., 1997. A GCM simulation of the climate 6000 years ago. J. Clim. 10, 3–17.

Hazeleger, W., Severijns, C., Semmler, T., Stefanescu, S., Yang, S., Wyser, K., Wang, X., Dutra, E., Baldasano, J.M., Bintanja, R., Bougeault, P., Caballero, R., Ekman, A.M., Christensen, J.H., van den Hurk, B., Jimenez, P., Jones, C., Kallberg, P., Koenigk, T., McGrath, R., Miranda, P., van Noije, T., Palmer, T., Parodi, J.A., Schmith, T., Selten, F., Storelvmo, T., Sterl, A., Tapamo, H., Vancoppenolle, M., Viterbo, P., Willen, U., 2010. EC-Earth: a seamless earth system prediction approach in action. Bull. Am. Meteorol. Soc. 91, 1357–1363.

Hazeleger, W., Wang, X., Severijns, C., Stefanescu, S., Bintanja, R., Sterl, A., Wyser, K., Semmler, T., Yang, S., van den Hurk, B., van Noije, T., van der Linden, E., van der Wiel, K., 2011. EC-Earth V2.2: description and validation of a new seamless earth system prediction model. Clim. Dyn. http://dx.doi.org/10.1007/s00382-011-1228-5.

Hennekam, R., Jilbert, T., Schnetger, B., de Lange, G.J., 2014. Solar forcing of Nile discharge and sapropel S1 formation in the early to middle Holocene eastern Mediterranean. Paleoceanography 29, 343–356. http://dx.doi.org/10.1002/2013PA002553.

Herold, M., Lohmann, G., 2009. Eemian tropical and subtropical African moisture transport: an isotope modelling study. Clim. Dyn. 33, 1075–1088.

Hoelzmann, P., Jolly, D., Harrison, S., Laarif, F., Bonnefille, R., Pachur, H.-J., 1998. Mid-Holocene land-surface conditions in northern Africa and the Arabian Peninsula: a data set for the analysis of biogeophysical feedbacks in the climate system. Glob. Biogeochem. Cycles 12, 35–51.

Kanarska, Y., Maderich, V., 2008. Modelling of seasonal exchange flows through the Dardanelles Strait, Estuarine. Coast. Shelf Sci. 79, 449–458.

Kaspar, F., Spangehl, T., Cubasch, U., 2007. Northern hemisphere winter storm tracks of the Eemain interglacial and the last glacial inception. Clim. Past 3, 181–192.

Kolodny, Y., Stein, M., Machlus, M., 2005. Sea-rain-lake relation in the Last Glacial East Mediterranean revealed by $\delta^{18}O$-δ^{13} C in Lake Lisan aragonites. Geochim. Cosmochim. Acta 69, 4045–4060.

Krinner, G., Lézine, A.-M., Braconnot, P., Sepulchre, P., Ramstein, G., Grenier, C., Gouttevin, I., 2012. A reassessment of lake and wetland feedbacks on the North African Holocene climate. Geophys. Res. Lett. 39.

Kutzbach, J.E., Chen, G., Cheng, H., Edwards, R., Liu, Z., 2013. Potential role of winter rainfall in explaining increased moisture in the Mediterranean and Middle East during periods of maximum orbitally-forced insolation seasonality. Clim. Dyn. http://dx.doi.org/10.1007/s00382-013-1692-1.

Larrasoaña, J.C., Roberts, A.P., Rohling, E.J., 2013. Dynamics of green Sahara periods and their role in hominin evolution. PLoS One 8, e76 514.

Levis, S., Bonan, G.B., Bonfils, C., 2004. Soil feedback drives the mid-Holocene North African monsoon northward in fully coupled CCSM2 simulations with a dynamic vegetation model. Clim. Dyn. 23, 791–802. http://dx.doi.org/10.1007/s00382-004-0477-y.

Lolis, C.J., Bartzokas, A., Katsoulis, B.D., 2002. Spatial and temporal 850 hPa air temperature and sea-surface temperature covariances in the Mediterranean region and their connection to atmospheric circulation. Int. J. Climatol. 22, 663–676. http://dx.doi.org/10.1002/joc.759.

Lourens, L.J., Antonarakou, A., Hilgen, F.J., Hoof, A.A.M.V., Zachariasse, W.J., 1996. Evaluation of the Plio-Pleistocene astronomical timescale. Paleoceanography 11, 391–413.

Ludwig, W., Dumont, E., Meybeck, M., Heussner, S., 2009. River discharges of water and nutrients to the Mediterranean and Black Sea: major drivers for ecosystem changes during past and future decades? Prog. Oceanogr. 80, 199–217.

Madec, G., 2008. NEMO Ocean Engine, p. 2008. Tech. rep., Institut Pierre-Simon Laplace, note du Pole de modelisation de l'Institut Pierre-Simon Laplace No 27.

Marino, G., Rohling, E.J., Rijpstra, W.I.C., Sangiorgi, F., Schouten, S., Damsté, J.S.S., 2007. Aegean Sea as driver of hydrographic and ecological changes in the eastern Mediterranean. Geology 35, 675–678.

Matthews, A., Ayalon, A., Bar-Matthews, M., 2000. *D/H* ratios of fluid inclusions of Soreq cave (Israel) speleothems as a guide to the Eastern Mediterranean Meteoric Line relationships in the last 120 ky. Chem. Geol. 166, 183–191.

Meijer, P.T., Tuenter, E., 2007. The effect of precession-induced changes in the Mediterranean freshwater budget on circulation at shallow and intermediate depth. J. Mar. Syst. 68, 349–365. http://dx.doi.org/10.1016/j.jmarsys.2007.01.006.
Osborne, A., Marino, G., Vance, D., Rohling, E., 2010. Eastern Mediterranean surface water Nd during Eemian sapropel S5: monitoring northerly (mid-latitude) versus southerly (sub-tropical) freshwater contributions. Quat. Sci. Rev. 29, 2473–2483.
Osborne, A.H., Vance, D., Rohling, E.J., Barton, N., Rogerson, M., Fello, N., 2008. A humid corridor across the Sahara for the migration of early modern humans out of Africa 120,000 years ago. Proc. Natl. Acad. Sci. 105, 16 444–16 447. http://dx.doi.org/10.1073/pnas.0804472105.
Pachur, H.-J., Braun, G., 1980. The paleoclimate of the Central Sahara, Libya, and the Libyan Desert. In: Sarnthein, M., Seibold, E., Rognon, P. (Eds.), Palaeoecology of Africa. Sahara and Surrounding Seas. A.A. Balkema, Rotterdam, pp. 351–363.
Paillou, P., Schuster, M., Tooth, S., Farr, T., Rosenqvist, A., Lopez, S., Malezieux, J.-M., 2009. Mapping of a major paleodrainage system in eastern Libya using orbital imaging radar: the Kufrah River. Earth Planet. Sci. Lett. 277, 327–333.
Paillou, P., Tooth, S., Lopez, S., 2012. The Kufrah paleodrainage system in Libya: a past connection to the Mediterranean Sea? Comptes Rendus Geosci. 344, 406–414.
Rachmayani, R., Prange, M., Schulz, M., 2015. North African vegetation-precipitation feedback in early and mid-Holocene climate simulations with CCSM3-DGVM. Clim. Past 11, 175–185.
Roberts, N., Jones, M., Benkaddour, A., Eastwood, W., Filippi, M., Frogley, M., Lamb, H., Leng, M., Reed, J., Stein, M., et al., 2008. Stable isotope records of Late Quaternary climate and hydrology from Mediterranean lakes: the ISOMED synthesis. Quat. Sci. Rev. 27, 2426–2441.
Rohling, E., Cane, T., Cooke, S., Sprovieri, M., Bouloubassi, I., Emeis, K., Schiebel, R., Kroon, D., Jorissen, F., Lorre, A., et al., 2002. African monsoon variability during the previous interglacial maximum. Earth Planet. Sci. Lett. 202, 61–75.
Rohling, E., Sprovieri, M., Cane, T., Casford, J., Cooke, S., Bouloubassi, I., Emeis, K., Schiebel, R., Rogerson, M., Hayes, A., et al., 2004. Reconstructing past planktic foraminiferal habitats using stable isotope data: a case history for Mediterranean sapropel S5. Mar. Micropaleontol. 50, 89–123.
Rohling, E., Abu-Zied, R., Casford, J., Hayes, A., Hoogakker, B., 2009. The marine environment: present and past. In: Woodward, J. (Ed.), The Physical Geography of the Mediterranean. Oxford University Press, Oxford, p. 33.
Rohling, E.J., 1994. Review and new aspects concerning the formation of eastern Mediterranean sapropels. Mar. Geol. 122, 1–28.
Rohling, E.J., Hilgen, F.J., 1991. The eastern Mediterranean climate at times of sapropel formation: a review. Geol. Mijnb. 70, 253–264.
Rohling, E.J., Marino, G., Grant, K., 2015. Mediterranean climate and oceanography, and the periodic development of anoxic events (sapropels). Earth-Sci. Rev. 143, 62–97.
Romem, M., Ziv, B., Saaroni, H., 2007. Scenarios in the development of Mediterranean cyclones. Adv. Geosci. 12, 59–65.
Rossignol-Strick, M., 1985. Mediterranean Quaternary sapropels, an immediate response of the African monsoon to variation of insolation. Palaeogeogr. Palaeoclimatol. Palaeoecol. 49, 237–263.
Rossignol-Strick, M., 1987. Rainy periods and bottom water stagnation initiating brine accumulation and metal concentrations: 1. The late Quaternary. Paleoceanography 2, 333–360.
Ruddiman, W.F., 2007. Earth's Climate: Past and Future. W.H. Freeman.
Saaroni, H., Bitan, A., Alpert, P., Ziv, B., 1996. Continental polar outbreaks into the Levant and eastern Mediterranean. Int. J. Climatol. 16, 1175–1191.
Sierro, F.J., Ledesma, S., Flores, J., Torrescusa, S., Martinez del Olmo, W., 2000. Sonic and gamma-ray astrochronology: cycle to cycle calibration of Atlantic climatic records to Mediterranean sapropels and astronomical oscillations. Geology 28, 695–698.
Soto-Navarro, F.J., Criado-Aldeanueva, F., Garcia-Lafuente, J., Sanchez-Roman, A., 2010. Estimation of the Atlantic inflow through the Strait of Gibraltar from Climatological and in situ data. J. Geophys. Res. 115 http://dx.doi.org/10.1029/2010JC006302.
Sterl, A., Bintanja, R., Brodeau, L., Gleeson, E., Koenigk, T., Schmith, T., Semmler, T., Severijns, C., Wyser, K., Yang, S., 2011. A look at the ocean in the EC-Earth climate model. Clim. Dyn. http://dx.doi.org/10.1007/s00382-011-1239-2.
Timm, O., Kohler, P., Timmermann, A., Menviel, L., 2010. Mechanisms for the onset of the African humid period and Sahara greening 14.5–11 ka BP. J. Clim. 23, 2612–2633.
Trigo, I.F., Davies, T.D., Bigg, G.R., 1999. Objective climatology of cyclones in the Mediterranean Region. J. Clim. 12, 1685–1696.
Tuenter, E., Weber, S.L., Hilgen, F.J., Lourens, L.J., 2003. The response of the African summer monsoon to remote and local forcing due to precession and obliquity. Glob. Planet. Change 36, 219–235. http://dx.doi.org/10.1016/S0921-8181(02)00196-0.
Tzedakis, P., 2009. Cenozoic climate and vegetation change. In: Woodward, J. (Ed.), The Physical Geography of the Mediterranean. Oxford University Press, Oxford, pp. 89–137.
Tzedakis, P.C., 2007. Seven ambiguities in the Mediterranean palaeoenvironmental narrative. Quat. Sci. Rev. 26, 2042–2066.
Ulbrich, U., Lionello, P., Belusic, D., Jacobeit, J., Knippertz, P., Kuglitsch, F.G., Leckebusch, G.C., Luterbacher, J., Maugeri, M., Maheras, P., Nissen, K.M., Pavan, V., Pinto, J.G., Saaroni, H., Seubert, S., Toreti, A., Xoplaki, E., Ziv, B., 2012. Climate of the Mediterranean: synoptic patterns, temperature, precipitation, winds, and their extremes. In: Lionelli, P. (Ed.), The Climate of the Mediterranean Region: from Past to the Future. Elsevier, pp. 301–346.
Valcke, S., Morel, T., 2006. OASIS3 User Guide. Tech. rep., CERFACS, prism Technical Report, p. 68. available online at: http://www.prism.enes.org/Publications/Reports/oasis3_UserGuide_T3.pdf.
van der Laan, E., Hilgen, F.J., Lourens, L.J., Kaenel, E. d., Gaboardi, S., Iaccarino, S., 2012. Astronomical forcing of Northwest African climate and glacial history during the late Messinian (6.55.5 Ma). Palaeoceanogr. Palaeoclimatol. Palaeoecol. 313–314, 107126. http://dx.doi.org/10.1029/2003PA000995.
Weldeab, S., Menke, V., Schmiedl, G., 2014. The pace of East African monsoon evolution during the Holocene. Geophys. Res. Lett. 41 http://dx.doi.org/10.1002/2014GL059361.
Xie, P., Arkin, P.A., 1997. Global precipitation: a 17-Year monthly analysis based on gauge observations, satellite estimates, and numerical model outputs. Bull. Am. Meteorol. Soc. 78, 2539–2558.
Xoplaki, E., Gonzalez-Rouco, J., Luterbacher, J., Wanner, H., 2004. Wet season Mediterranean precipitation variability: influence of large-scale dynamics and trends. Clim. Dyn. 23, 63–78.